science, engineering and health studies

Research Article

Science, Engineering and Health Studies
https://lio1.tci-thaijo.org/index.php/sehs
ISSN (Online): 2630-0087

Optimization of nanocrystalline cellulose particle size using one-factor-at-a-time method under different acid hydrolysis parameters

Chu Yong Soon[1], Carine Shu Shien Lim[1], Yonchen Hariyanto[1], Rosnita Abdul Talib[2], Khalina Abdan[3,4], Chen Wai Wong[1], and Eric Wei Chiang Chan[5]*

[1] Faculty of Applied Sciences, UCSI University, 56000, Kuala Lumpur, Malaysia
[2] Department of Process and Food Engineering, Faculty of Engineering, Universiti Putra Malaysia, 43400, Selangor, Malaysia
[3] Department of Biological and Agricultural Engineering, Faculty of Engineering, Universiti Putra Malaysia, 43400, Selangor, Malaysia
[4] Laboratory of Biocomposite Technology, Institute of Tropical Forestry and Forest Products (INTROP), Universiti Putra Malaysia, 43400, Selangor, Malaysia
[5] Sustainable Coastal Cities Research Consortium, UCSI University, 56000, Kuala Lumpur, Malaysia

***Corresponding author**: Eric Wei Chiang Chan
chanwc@ucsiuniversity.edu.my*

***Received**: 17 January 2023*
***Revised**: 19 May 2023*
***Accepted**: 8 July 2023*
***Published**: 16 November 2023*

***Citation**: Soon, C. Y., Lim, C. S. S., Hariyanto, Y., Talib, R. A., Abdan, K., Wong, C. W., and Chan, E. W. C. (2023). Optimization of nanocrystalline cellulose particle size using one-factor-at-a-time method under different acid hydrolysis parameters. Science, Engineering and Health Studies, 17, 23030001.*

ABSTRACT

This study explores the production of nanocrystalline cellulose (NCC) from corn cob (Zea mays), aiming to overcome the challenges of carbonization and reduced yield typically associated with the use of highly concentrated and corrosive sulfuric acid. A systematic approach was adopted employing one-factor-at-a-time analysis to optimize the hydrolysis process, focusing on three key parameters: sulfuric acid concentration, hydrolysis temperature, and duration. The determination of optimized conditions was based on the desired particle size of the NCC produced and the absence of carbonization. The produced NCC was thoroughly characterized using Fourier transform infrared spectroscopy to determine its chemical structure, X-ray diffraction for crystallinity, and thermogravimetric analysis (TGA) for thermal properties. The results highlighted that the optimal conditions for NCC production involve a sulfuric acid concentration of 40 wt% at a temperature of 70 °C, with a hydrolysis duration of 150 min. These conditions yielded NCC with a uniform particle size of 225.07 nm, no signs of carbonization, and a significantly lower inorganic content at 6.73 w/w% after heating to 590 °C in the TGA. This study thereby offers valuable insights for producing NCC with reduced carbonization and increased yield.

Keywords: nanocrystalline cellulose; one-factor-at-a-time; acid hydrolysis; carbonization

1. INTRODUCTION

Cellulose, the most abundant natural polymer in the world, is a challenging material to break down due to its strong hydrogen bonding (Pandey, 2017). Its nanoscale derivative, nanocellulose, forms a negative electrostatic layer due to negatively charged groups, promoting its dispersion in water and ensuring its thermostability (Grande et al., 2017). This nanomaterial is particularly promising as a reinforcement for polymers due to the potent effects of its interfibre hydrogen bonds, which are not present in microfiber composites (Thomas et al., 2018).

However, the strength and modulus of nanocellulose composites increase only up to an optimal content of about 5%, after which further nanocellulose content results in impairment (Azeredo et al., 2017).

The production of cellulose, and subsequently nanocellulose, can be achieved using lignocellulosic material. The process starts with delignification and hemicellulose removal to produce microcellulose. Conversion from microcellulose to nanocrystalline cellulose (NCC) is typically performed through an acid hydrolysis method with sulfuric acid due to its consistent performance and short reaction time (Adriana et al., 2020). This process introduces sulphate groups to the NCC through the catalytic degradation of sulfuric acid.

The current standard method for producing NCC via hydrolysis involves a 60–64% sulfuric acid solution heated at 45 °C for 45–60 min (Naduparambath et al., 2018). However, under these conditions, NCC often undergoes carbonization, a process that transforms biomass into a carbonaceous solid when exposed to an aqueous catalyst (Han et al., 2022). Although this carbonization results in porous cellulose with coal fuel, electrode material, sorbent, and catalyst applications, it reduces the material's utility as a polymeric filler (Burra et al., 2021; Heidarinejad et al., 2020).

This research seeked to address this issue by proposing a set of guidelines to design acid hydrolysis parameters that optimize NCC particle size while preventing carbonization. It suggests milder hydrolysis conditions using a lower concentration of sulfuric acid, with extended temperature and reaction duration (Heidarinejad et al., 2020). This method provides a buffer period for the observation of any immediate carbonization reactions that could damage the NCC.

The present study utilized corn cob (*Zea mays*) as a cellulose feedstock for the production of NCC (Sumaila et al., 2020). To achieve this optimization, the study employed the one-factor-at-a-time (OFAT) approach. This systematic scientific method evaluated parameters such as sulfuric acid concentration, hydrolysis temperature, and hydrolysis duration. The physicochemical and thermal properties of the resulting NCC were also characterized as part of the study.

2. MATERIALS AND METHODS

2.1 Materials

Corn cob (*Zea mays*) was provided by Marine Gold Marketing Sdn. Bhd., Malaysia. A commercial cellulose nanocrystal (cNCC), used as the control in this study, was purchased from Cellulose Lab, Canada. The chemicals used, including sodium chlorite ($NaClO_2$), acetic acid (CH_3COOH), sodium hydroxide (NaOH), hydrochloric acid (HCl), and sulfuric acid (H_2SO_4), were all of analytical grade.

2.2 Microcrystalline cellulose (MCC) production from corn cob

Corn cob was dried, blended, and then sieved to obtain a powder with a particle size ranging between 250 µm and 500 µm. This powder was then bleached using a 5% w/v solution of $NaClO_2$ in a ratio of 1:10. The bleaching process was activated by the addition of 1 mL of concentrated CH_3COOH for every 100 mL of $NaClO_2$ used, and the mixture was heated at 80 °C for 2 h (Fortunati et al., 2013).

Following this, the delignification process resulted in a cellulose pulp, which was subsequently filtered and washed with deionized water. To remove the hemicellulose content, the pulp was hydrolysed further using a 20% w/v solution of NaOH. This was performed at boiling temperature for 3 h, with continuous stirring (Fahma et al., 2010). Finally, the MCC was washed until it reached a neutral pH.

2.3 NCC optimization from MCC

OFAT method was used to analyze the production of NCC using sulfuric acid hydrolysis. This process involved a series of steps, starting with the mixing of MCC powder with sulfuric acid in a 1:20 ratio under continuous stirring.

Hydrolysis was initially conducted at varying temperatures, ranging from 40–80 °C, while maintaining a fixed sulfuric acid concentration and hydrolysis duration. Once the optimum temperature was determined, it was kept constant for subsequent tests, during which the sulfuric acid concentration varied from 20–50 wt%. This was done while preserving the same hydrolysis duration as in the previous temperature test.

In the next stage, both the optimized temperature and sulfuric acid concentration were utilized to find the ideal hydrolysis duration, testing intervals from 50–200 min. These optimization steps were guided by the goal of achieving the best particle size for the produced NCCs. After the acid hydrolysis process, the NCC pulp was washed multiple times through centrifugation before being freeze-dried. Each treatment was replicated three times over two separate batches to ensure reliability of the results.

2.4 Particle size analysis

A 0.5% suspension of NCC was prepared by thoroughly homogenizing freeze-dried NCC powder in water. This was accomplished using an ultrasound homogenizer. The particle size of the NCC in the suspension was then determined using a particle size analyzer, specifically the Malvern Zetasizer Nano ZS from the UK. For this process, the reflection index of the NCC in the water suspension was set at 1.510.

2.5 Physicochemical and thermal properties

The chemical compositions of the NCC samples were determined through characterization using transform infrared spectroscopy, utilizing a Thermo Scientific Nicolet iS5 from the USA and the attenuated total reflectance (ATR) technique. The FT-IR spectrum was recorded within a wavelength range of 400 cm^{-1} to 4000 cm^{-1}, employing a spectral resolution of 4 cm^{-1}. A total of 64 scans were completed for each sample.

In addition, X-ray diffraction analysis was performed using a Shimadzu XRD-6000. The XRD settings were at 30 kV and 30 mA, with a 2θ scan angle range from 5° to 45°, employing Cu-Kα radiation (λ=1.5406 Å). The degree of crystallinity (X_{cr}) was determined based on the area ratio of the crystal phase to the sum of the crystal and amorphous phases in the XRD diagram, calculated using Equation 1.

$$X_{cr}(\%) = \left(I_{(110)} - I_{(020)}\right)/I_{(110)} \times 100 \qquad (1)$$

where $I_{(110)}$ is the maximum/peak intensity at a 2θ angle of crystalline material and $I_{(020)}$ is the maximum/peak intensity at a 2θ angle of amorphous material.

The thermal degradation properties of the NCC samples were evaluated using a Thermo-gravimetric analyser, specifically a Perkin Elmer, TGA 7, USA model. Each sample, weighing approximately 10 mg, was placed on the heating pan. The analysis was performed in the ramp mode, with a temperature range from 30–600 °C, applying a constant heating rate of 10 °Cmin. To prevent thermo-oxidative degradation, the tests were conducted under a nitrogen atmosphere, flowing at 20 mLmin.

2.6 Statistical analysis

The mean ± SD of the results from three replicates was calculated. The statistical difference was analyzed by one-way ANOVA using JMP Pro 12 with a confidence level of 0.95. A post-hoc Tukey-Kramer test (α = 0.05) was used to compare the significant difference between each formulation combination.

3. RESULTS AND DISCUSSION

3.1 Optimization of NCC particle size via OFAT

The OFAT analysis for the production of NCC targeted three parameters: hydrolysis temperature, sulfuric acid concentration, and hydrolysis duration. This was done to manage the effects of carbonization and achieve the desired particle size, as detailed in Table 1.

During the investigation of the temperature range (40–80 °C), using 30 wt% H_2SO_4 for 100 min, a significant difference was observed in the NCC particle size [F (4, 10)=31.9991, p<0.0001*]. As the hydrolysis temperature increased to 60 °C, the NCC particle size decreased substantially from about 4000 nm to 1383.67 ± 211.68 nm. This suggested that 60 °C is a critical temperature for minimizing the activation energy during acid hydrolysis. However, the produced NCCs demonstrated considerable variation and inconsistency in particle size. The high PDI of the NCC suspensions also indicated poor distribution and dispersion.

Regarding the sulfuric acid concentration, a notable decreasing trend was observed in the NCC particle size at varying acid concentrations (20–50% w/w) [F (3, 8)= 5.1252, p=0.0287*]. The smallest particle size was found in NCC-C50 (577.13 ± 58.76 nm) and it displayed a smaller standard deviation and PDI value, suggesting uniform hydrolysis. Yet, NCC-C50 displayed signs of darkening, indicating excessive hydrolysis and carbonization due to the high H_2SO_4 concentration. NCC-C40, however, showed no signs of carbonization, suggesting that the given concentration adequately degraded the amorphous domains of long cellulose microfibrils.

When optimizing the hydrolysis duration (ranging 50–200 min), with a fixed hydrolysis temperature of 70 °C and 40% w/w H_2SO_4 concentration, significant differences were noted in both particle size [F (3, 8) = 58.2491, p<0.0001*] and PDI [F (3, 8) = 39.9878, p<0.0001*] of the produced NCCs. NCC-t150, which showed no signs of carbonization, had the smallest particle size (225.07 ± 19.03 nm) and lowest PDI value (0.36 ± 0.06) among all the tested durations. This suggests that these conditions effectively hydrolyze cellulose. Although commercial NCC (cNCC) had a smaller particle size (68.87 ± 1.87 nm), its PDI value was higher (0.55 ± 0.03) than NCC-t150. Consequently, NCC-t150 outperformed cNCC due to its superior uniformity in particle size.

Table 1. Particle size and poly-dispersion index (PDI) estimation of NCCs

NCC sample	Temperature (°C)	H_2SO_4 (% w/w)	Duration (min)	Particle size (nm)	PDI
NCC-T40	40	30	100	3853.33 ± 657.06 ^{a}	1.00 ± 0.00 ^{a}
NCC-T50	50	30	100	3915.33 ± 280.71 ^{a}	1.00 ± 0.00 ^{a}
NCC-T60	60	30	100	1383.67 ± 211.68 ^{b}	1.00 ± 0.00 ^{a}
NCC-T70	70	30	100	1022.07 ± 505.23 ^{b}	0.92 ± 0.13 ^{ab}
NCC-T80	80	30	100	1726.67 ± 320.16 ^{b}	1.00 ± 0.00 ^{a}
NCC-C20	70	20	100	1364.33 ± 211.91 ^{a}	0.97 ± 0.03 ^{a}
NCC-C30	70	30	100	1022.07 ± 505.23 ^{ab}	0.92 ± 0.13 ^{ab}
NCC-C40	70	40	100	648.87 ± 82.69 ^{ab}	0.75 ± 0.09 ^{b}
NCC-C50	70	50	100	577.13 ± 58.76 ^{b}	0.71 ± 0.04 ^{b}
NCC-t50	70	40	50	1204.67 ± 165.53 ^{a}	0.98 ± 0.02 ^{a}
NCC-t100	70	40	100	648.87 ± 82.69 ^{b}	0.75 ± 0.09 ^{b}
NCC-t150	70	40	150	225.07 ± 19.03 ^{c}	0.36 ± 0.06 ^{c}
NCC-t200	70	40	200	453.23 ± 38.80 ^{bc}	0.88 ± 0.11 ^{ab}
cNCC	-	-	-	68.87 ± 1.87	0.55 ± 0.03

Note: a–c indicate significant difference (p<0.05) among the comparisons. NCCs are coded by temperature (T), concentration (C) and time (t).

3.2 Physicochemical properties analysis

The physicochemical properties of NCC were assessed using FT-IR and XRD. Representative cellulose samples, including delignified cellulose, MCC, NCC-C50, and NCC t150, were selected for FT-IR spectra analysis as presented in Figure 1(a).

The broad peak seen at 3333 cm^{-1} indicates the presence of O–H stretching, comprised of inter- and

intramolecular hydrogen bond vibrations in cellulose (Ma et al., 2015). The absence of the peak at 1728 cm^{-1} in MCC and the produced NCCs suggested the successful removal of the acetyl group's C=O stretching in hemicellulose during alkaline treatment.

Multiple peaks in the 1450–1300 cm^{-1} range were identified, including at 1428 cm^{-1} (-CH2 bending), 1369 cm^{-1} (-CH deformation), and 1316 cm^{-1} (-CH2 deformation) (Boukir et al., 2019). The signals found at 1428, 1159, 1103, and 1052 cm^{-1} confirmed the NCCs as cellulose type 1 (Fortunati et al., 2013). The absorption at 897 cm^{-1} further validated the NCC structure, revealing the presence of the critical functional group in the 1,4-glucosidic linkage between glucose units (Heidarian et al., 2016). XRD analysis, as demonstrated in Figure 1(b), (c) and (d), showed a sharp peak at 22°, representing the crystalline region with plane (002). Another peak was observed at 16°, indicative of the amorphous region with plane (101). The X_{cr} is determined by the intensity difference between crystalline and amorphous materials and the ratio of crystalline regions. An additional peak at 20.5° was found in cNCC, possibly corresponding to the amorphous region of cellulose, which is present in certain brands of cNCC, such as Avicel by Dupont, but absent in those derived from pulp (Yao et al., 2020). It is hypothesized that this could result from the addition of stabilizers like carboxymethyl cellulose in commercial preparations.

Recorded X_{cr} values for NCC-T50, NCC-t150, and cNCC were 40.52%, 59.33%, and 74.31%, respectively. The X_{cr} for NCC-T50 aligned with nanocellulose extracted from peach palm (Bactris gasipaes) (49.8–54.5%) and washed cotton cloth (55.76–62.67%) (Wang et al., 2017; Franco et al., 2019). Importantly, all observed peaks in the produced NCCs were consistent with the diffraction peaks of cellulose type 1, suggesting that the hydrolysis process did not impact the structure.

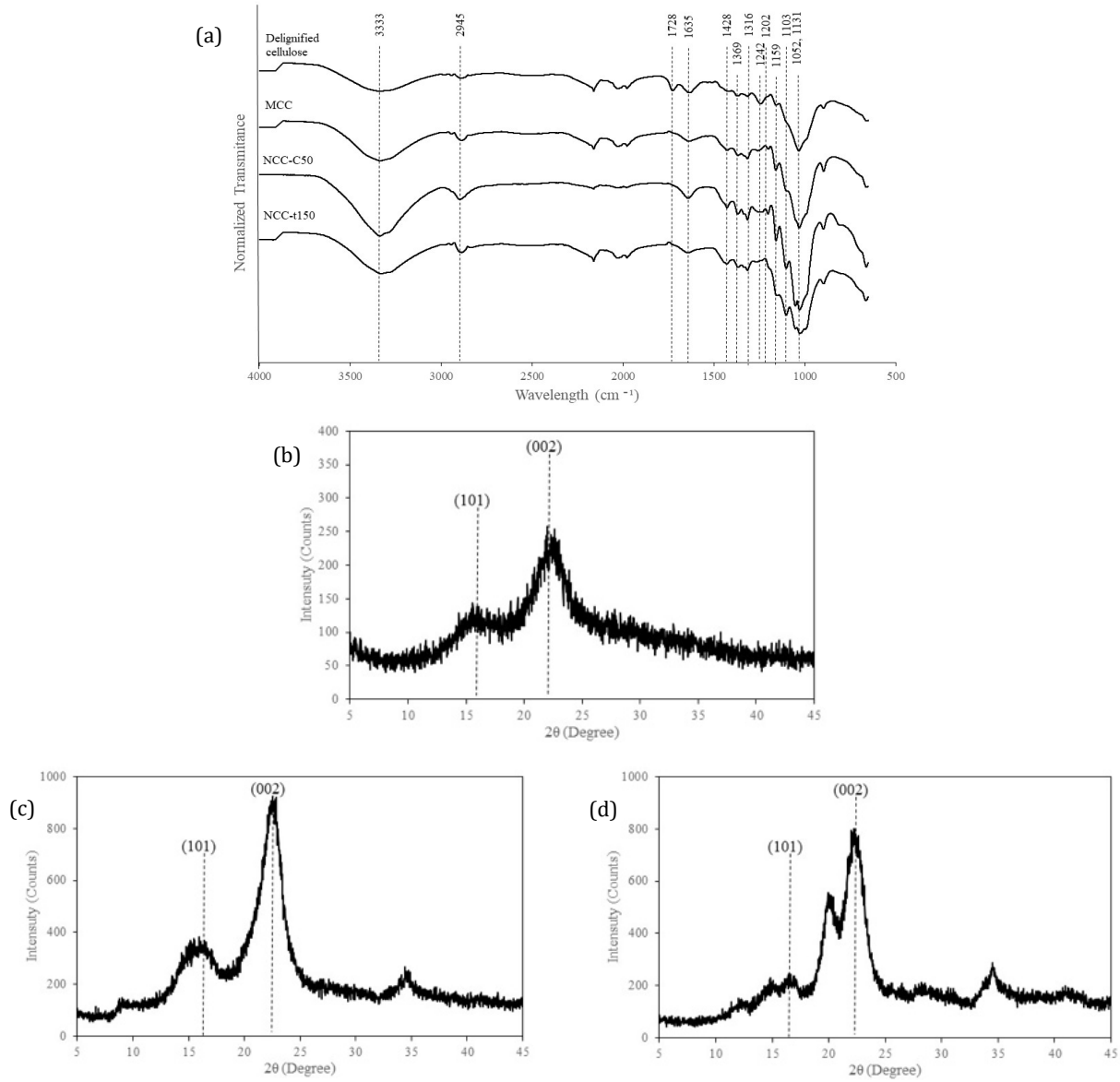

Figure 1. Attenuated FT-IR spectra of (a) cellulose samples and XRD diffractograms of (b) NCC-T50, (c) NCC-t150, and (d) cNCC with scanning angle from 5–45° scanning angle from 2°min scanning speed at 30 kV, 30 mA

3.3 Thermal properties of NCCs

The thermal degradation properties of various cellulose samples were assessed, as shown in Figure 2. All samples demonstrated the initial thermal degradation below 100 °C, which is associated with water evaporation, reflecting cellulose's hydrophilic tendency to adsorb ambient humidity. Major thermal degradation commenced at around 250 °C, coinciding with the combustion of most hydrocarbon compounds. This observation aligns with previous findings on cellulose pyrolysis, indicating processes such as water desorption and cellulose dehydration (below 150 °C), and the thermal cleavage of the glycosidic linkage, other carbon-oxygen bonds, and some carbon-carbon bonds (240–400 °C) (Tang and Bacon, 1964).

The maximum degradation temperature (T_{max}) was found to be highest for microcrystalline cellulose (MCC) at 339.77 °C. This was followed by NCC-t150 at 306.99 °C, commercial NCC (cNCC) at 290.59 °C, and NCC-C50 at 282.45 °C, being the lowest. The lower T_{max} of NCC-C50 could be related to its lower degree of crystallinity reported earlier. It has been noted that the thermal degradation of cellulose begins in amorphous regions and progresses to more crystalline regions (Adawiyah et al., 2022). Many studies have also reported the plateau region of nanocellulose's range to be between 280 °C and 400 °C, similar to nanocellulose from mulberry, sugarcane bagasse, and red algae (Chen et al., 2016).

$T_{10\%}$ refers to the temperature at which 10% of the dry weight content is lost due to progressive heating. All the cellulose samples exhibited $T_{10\%}$ within the range of 265 °C to 280 °C. The Tmax and $T_{10\%}$ findings suggest that MCC displays better thermal stability compared to the NCCs.

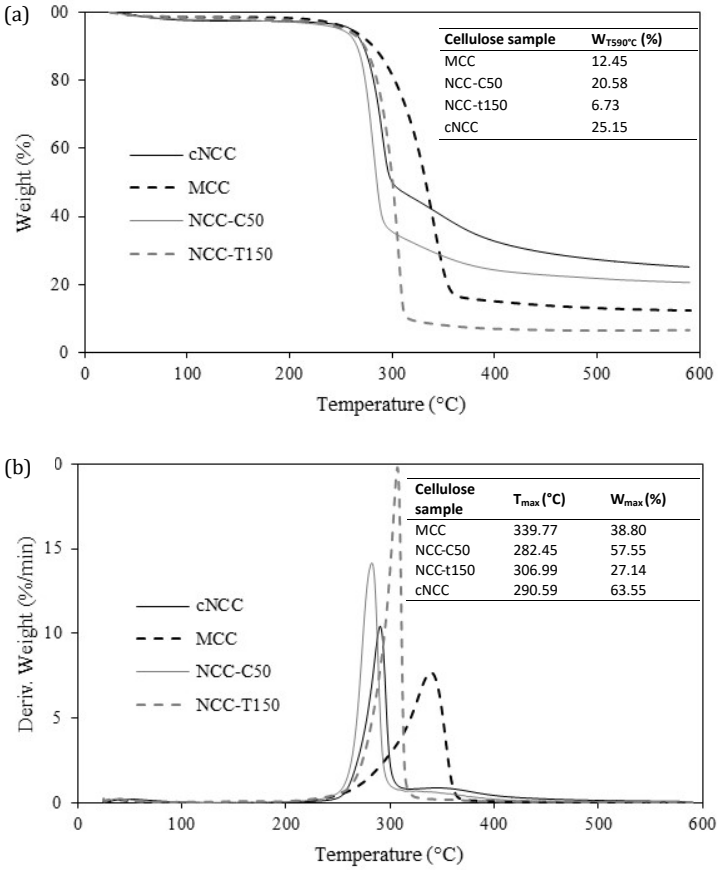

Figure 2. (a) TGA and (b) DTG of the thermal degradation process of different sizes of cellulose from 25–590 °C with 5 °C min^{-1} constant ramping under nitrogen environment

The weight remaining after heating the cellulose samples to 590°C, represented by $W_{T590\,°C}$, was expected to be relatively low for all samples. The highest $W_{T590\,°C}$ was found in cNCC at 25.15%, followed by NCC-C50 at 20.58%. Conversely, NCC-t150 reported the lowest $W_{T590\,°C}$ at 6.73%.

Cellulose, being composed of glucose monomers, is expected to leave behind 12–15% of carbon mass residue at 400 °C and even less than 10% at 1000°C (Ishida et al., 2004). The elevated $W_{T590\,°C}$ of NCC-C50 may be attributed to a high carbon content resulting from carbonization. For cNCC, the higher $W_{T590\,°C}$ could partially be due to mineral salt impurities. The notably low $W_{T590\,°C}$ of NCC-t150 suggests minimal char residue in the samples, which is considerably lower than what would typically be expected.

4. CONCLUSION

In conclusion, this study employed a systematic and straightforward approach to evaluate the feasibility of NCC production through acid hydrolysis while circumventing carbonization. Utilizing the OFAT analysis, optimized

conditions for the hydrolysis process were identified: a temperature of 70 °C, sulfuric acid concentration at 40 wt%, and a duration of 150 min. These conditions facilitated the generation of a batch of NCC, referred to as NCC-t150, that had a consistent particle size of 225.07 nm, a PDI of 0.36, and showed no signs of carbonization. To effectively hydrolyze cellulose into NCC while avoiding carbonization, the following guidelines are proposed based on the findings of this study:

1. Maintain the hydrolysis temperature at around 70 °C. Exceeding this limit may reduce the particle size but it may also accelerate carbonization.

2. Use a sulfuric acid concentration of 40 wt%. A higher concentration might cause excessive hydrolysis, leading to the darkening of the samples and increased carbonization.

3. Limit the hydrolysis duration to approximately 150 min. Prolonged exposure to the hydrolysis conditions may lead to unwanted changes in the cellulose structure, which might include carbonization.

While these guidelines assist in producing a desirable NCC batch, it is crucial to note that the desire for smaller particle sizes might necessitate carbonization. However, such an approach is less sustainable, requires higher acid concentrations, and necessitates an additional step to remove carbonized char. Future work should consider these aspects to ensure both the efficacy and sustainability of the hydrolysis process.

ACKNOWLEDGMENT

The authors gratefully acknowledge financial support from the Ministry of Higher Education (MOHE) Malaysia under the Fundamental Research Grant Scheme (FRGS) with grant code [FRGS-1-2022-STG04-UCSI-02-2].

REFERENCES

Adawiyah, R., Suryanti, V., and Pranoto. (2022). Preparation and characterization of *microcrystalline cellulose* from lembang (*Typha angustifolia* L.). *Journal of Physics: Conference Series*, 2190, 012007.

Adriana, A., Saifuddin, S., and Jalal, R. (2020). Production and characterization of nanocrystalline cellulose from palm empty fruit bunch fiber. *IOP Conference Series: Materials Science and Engineering*, 732, 012006.

Azeredo, H. M. C., Rosa, M. F., and Mattoso, L. H. C. (2017). Nanocellulose in bio-based food packaging applications. *Industrial Crops and Products*, 97, 664–671.

Boukir, A., Fellak, S., and Doumenq, P. (2019). Structural characterization of *Argania spinosa* Moroccan wooden artifacts during natural degradation progress using infrared spectroscopy (ATR-FTIR) and X-Ray diffraction (XRD). *Heliyon*, 5(9), e02477.

Burra, K. G., Daristotle, N., and Gupta, A. K. (2021). Carbonization of cellulose in supercritical CO_2 for value-added carbon. *Journal of Energy Resources Technology*, 143(7), 072105.

Chen, Y. W., Lee, H. V., Juan, J. C., and Phang, S.-M. (2016). Production of new cellulose nanomaterial from red algae marine biomass *Gelidium elegans*. *Carbohydrate Polymers*, 151, 1210–1219.

Fahma, F., Iwamoto, S., Hori, N., Iwata, T., and Takemura, A. (2010). Isolation, preparation, and characterization of nanofibers from oil palm empty-fruit-bunch (OPEFB). *Cellulose*, 17(5), 977–985.

Fortunati, E., Puglia, D., Monti, M., Peponi, L., Santulli, C., Kenny, J. M., and Torre, L. (2013). Extraction of cellulose nanocrystals from *Phormium tenax* fibres. *Journal of Polymers and the Environment*, 21(2), 319–328.

Franco, T. S., Potulski, D. C., Viana, L. C., Forville, E., de Andrade, A. S., and de Muniz, G. I. B. (2019). Nanocellulose obtained from residues of peach palm extraction (*Bactris gasipaes*). *Carbohydrate Polymers*, 218, 8–19.

Grande, R., Trovatti, E., Carvalho, A. J. F., and Gandini, A. (2017). Continuous microfiber drawing by interfacial charge complexation between anionic cellulose nanofibers and cationic chitosan. *Journal of Materials Chemistry A*, 5(25), 13098–13103.

Han, S., Bai, L., Chi, M., Xu, X., Chen, Z., and Yu, K. (2022). Conversion of waste corn straw to value-added fuel via hydrothermal carbonization after acid washing. *Energies*, 15(5), 1828.

Heidarian, P., Behzad, T., and Karimi, K. (2016). Isolation and characterization of bagasse cellulose nanofibrils by optimized sulfur-free chemical delignification. *Wood Science and Technology*, 50(5), 1017–1018.

Heidarinejad, Z., Dehghani, M. H., Heidari, M., Javedan, G., Ali, I., and Sillanpää, M. (2020). Methods for preparation and activation of activated carbon: a review. Environmental Chemistry Letters, 18(2), 393–415.

Ishida, O., Kim, D.-Y., Kuga, S., Nishiyama, Y., and Brown, R. M. (2004). Microfibrillar carbon from native cellulose. *Cellulose*, 11, 475–480.

Ma, Z., Pan, G., Xu, H., Huang, Y., and Yang, Y. (2015). Cellulosic fibers with high aspect ratio from cornhusks via controlled swelling and alkaline penetration. *Carbohydrate Polymers*, 124, 50–56.

Naduparambath, S., Jinitha T. V., Shaniba, V., Sreejith, M. P., S., Balan, A. K., and Purushothaman, E. (2018). Isolation and characterisation of cellulose nanocrystals from sago seed shells. *Carbohydrate Polymers*, 180, 13–20.

Pandey, S. (2017). A comprehensive review on recent developments in bentonite-based materials used as adsorbents for wastewater treatment. *Journal of Molecular Liquids*, 241, 1091–1113.

Sumaila, A., Ndamitso, M. M., Iyaka, Y. A., Abdulkareem, A. S., Tijani, J. O., and Idris, M. O. (2020). Isolation and characterization of selected biopolymers from Maize Cobs and Crab Shells obtained in Niger State, Nigeria. *Research Journal of Material Sciences*, 8(1), 19–23.

Tang, M. M., and Bacon, R. (1964). Carbonization of cellulose fibers—I. low temperature pyrolysis. *Carbon*, 2(3), 211–214.

Thomas, B., Raj, M. C., Athira, K. B., Rubiyah, M. H., Joy, J., Moores, A., Drisko, G. L., and Sanchez, C. (2018). Nanocellulose, a versatile green platform: From biosources to materials and their applications. *Chemical Reviews*, 118(24), 11575–11625.

Wang, Z., Yao, Z., Zhou, J., and Zhang, Y. (2017). Reuse of waste cotton cloth for the extraction of cellulose nanocrystals. *Carbohydrate Polymers*, 157, 945–952.

Yao, W., Weng, Y., and Catchmark, J. M. (2020). Improved cellulose X-ray diffraction analysis using Fourier series modeling. *Cellulose*, 27, 5563–5579.